ACS OMEGA

http://pubs.acs.org/journal/acsodf

Article

Evaluation of Silicone Fluids and Resins as CO_2 Thickeners for Enhanced Oil Recovery Using a Computational and Experimental Approach

Gonzalo Gallo, Eleonora Erdmann, and Claudio N. Cavasotto*

Cite This: *ACS Omega* 2021, 6, 24803−24813

Read Online

ACCESS | Metrics & More | Article Recommendations

ABSTRACT: CO_2 thickeners have the potential to be a game changer for enhanced oil recovery, carbon capture utilization and storage, and hydraulic fracturing. Thickener design is challenging due to polymers' low solubility in supercritical CO_2 ($scCO_2$) and the difficulty of substantially increasing the viscosity of CO_2. In this contribution, we present a framework to design CO_2 soluble thickeners, combining calculations using a quantum mechanical solvation model with direct laboratory viscosity testing. The conductor-like polarizable continuum model for solvation free-energy calculations was used to determine functional silicone and silsesquioxane solubilities in $scCO_2$. This method allowed for a fast and efficient identification of CO_2-soluble compounds, revealing silsesquioxanes as more CO_2-philic than linear polydimethylsiloxane (PDMS), the most efficient non-fluorinated thickener know to date. The rolling ball apparatus was used to measure the viscosity of $scCO_2$ with both PDMS and silicone resins with added silica nanoparticles. Methyl silicone resins were found to be stable and fast to disperse in $scCO_2$ while having a significant thickening effect. They have a larger effect on the solution viscosity than higher-molecular-weight PDMS and are able to thicken CO_2 even at high temperatures. Silicone resins are thus shown to be promising $scCO_2$ thickeners, exhibiting enhanced solubility and good rheological properties, while also having a moderate cost and being easily commercially attainable.

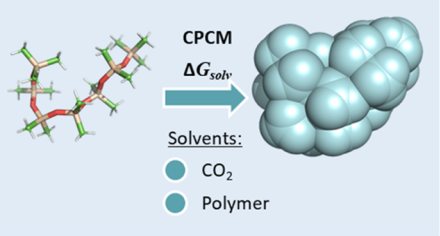

■ INTRODUCTION

CO_2 injection is one of the most broadly used enhanced oil recovery (EOR) technologies worldwide. Under reservoir conditions, CO_2 is in the supercritical state ($scCO_2$) and has a liquid-like density while exhibiting a gas-like viscosity. The significant viscosity gap between oil and the solvent may lead to viscous fingering, channeling the gas, and impairing the areal extension of the injected slug, therefore compromising the macroscopic sweep efficiency.

Water alternating gas (WAG) is the most broadly used method for improving macroscopic sweep efficiency in CO_2 EOR. Nonetheless, injecting different phases could generate problems like water blocking, especially at high water saturations.[1−3] The CO_2-rich phase may not contact the oil in smaller pores due to capillary pressure creating a capillary induced bypassing.[4] While volumetric efficiency is enhanced by higher WAG ratios, reduced WAG ratios or even continuous CO_2 injection can have a positive effect on microscopic efficiency.[5] In order to obtain both good microscopic and macroscopic sweep efficiency, CO_2 thickeners could be used as a mobility control agent.

Another operational issue observed in various CO_2 EOR projects is injectivity reduction due to changes in relative permeabilities.[6] Both CO_2 and water injectivities have shown to decrease in WAG and simultaneous water-gas injection. In the Grayburg formation (Permian Basin), a water injectivity loss of up to 90% has been reported.[7] The loss of injectivity derives in a significant pressure drop around the wellbore, reducing the overall reservoir pressure, and miscibility conditions may be lost. It is possible to reduce injectivity loss effects by increasing the gas slug size in WAG cycles,[6] and by utilizing thickeners alongside with larger gas slugs, volumetric efficiency could be maintained. Furthermore, water availability or water quality issues can also be of concern in some regions. Enhancement of CO_2 viscosity would allow reducing water utilization and all its related issues while maintaining sweep efficiencies.

An affordable CO_2 thickener solution is today acknowledged as a game-changing technology since it would have profound effects on oil recovery.[8] Such a mobility control agent would adjust the CO_2-rich solution's viscosity by simply varying its concentration. By directly increasing the viscosity of the CO_2 phase, mobility control can be obtained regardless of the relative permeability of the rock, fluid saturations, or brine properties. Viscosity enhancement has been attained by using

Received: July 11, 2021
Published: September 13, 2021

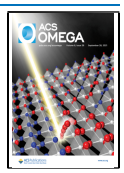

https://doi.org/10.1021/acsomega.1c03660
ACS Omega 2021, 6, 24803−24813

CO_2-soluble surfactants and polymers (with and without co-solvents) and most recently with nanoparticles.

Bae and Irani pioneered CO_2 thickener research by utilizing high-molecular-weight (MW) polydimethylsiloxane (PDMS), with toluene as a co-solvent; this formulation has proven to increase CO_2 viscosity up to 90-fold. A 6, 4, and 2 wt % polymer solution in CO_2 increased its viscosity to 3.48, 1.2, and 0.8 cp, respectively, under reservoir conditions. While thickened CO_2 was shown to improve oil recovery from cores and increase gas viscosity, the co-solvent (toluene) requirement made pilot-testing costs prohibitive.[9] Silicones have also been used as thickeners for fracturing fluids with utilization of kerosene as a co-solvent.[10] Functional silicones with anthraquinone-2-carboxamide end groups,[11] ester, amide, urea functional groups,[12] epoxy-terminated PDMS,[13] and epoxy ether-based PDMS were tested as thickeners for CO_2-based fluids,[14,15] but all had limited solubility. Branched siloxanes were found to have a higher solubility in $scCO_2$ than linear silicones.[12] Copolymers based on epoxide heptamethyltrisiloxane and glycidyl phenyl ether also showed to increase CO_2 viscosity.[16]

Fluorinated thickeners were successfully developed for CO_2. Formulations such as a fluorinated telechelic ionomer, a tri(semi-fluorinated alkyl) tin fluoride, a surfactant with two twin-tailed fluorinated tails, and a high-MW fluoroacrylate homopolymer have been evaluated.[8,17] Poly (fluoroacrylate-styrene) is a fluorinated compound that was able to increase CO_2 viscosity by 10-fold and 19-fold with under 1 and 1.5 wt % additive concentrations, respectively.[18] A four-armed oligomeric CO_2 thickener containing fluorine was recently developed significantly increasing carbon dioxide's viscosity.[19] Unfortunately, fluorinated compounds are expensive and carry health and environmental concerns.

Recently, nanoparticles have been used to improve EOR methods. Mixture or chemical EOR with nanoparticles has been utilized in water-based nanofluids as well to enhance their physical properties.[20] Shah (2009) dispersed CuO nanoparticles in CO_2 with PDMS as a co-solvent. The formulation obtained had a 2.28 cp viscosity under reservoir conditions and showed significant incremental oil recovery in core floods. They additionally developed a formulation with viscosity-reducing injectants.[21] Hashemi et al. (2016) used NiO nanoparticles with PDMS as a co-solvent. NiO nanoparticles were able to destabilize asphaltene depositions in porous media, mitigating permeability reduction and achieving a significant improvement in the final oil recovery.[22] Jafari et al. (2015) used water as a co-solvent to disperse silica nanoparticles in CO_2. The use of water to disperse the nanoparticles in CO_2 significantly reduced the costs, although oil recovery factor increment was not as significant as in the other formulations. WAG with nanoparticle-saturated CO_2 was also tested with positive results.[23] Recently, computational models on MatLab were used to determine optimal nanoparticle concentration in CO_2 EOR.[24] Also, the graphene oxide/P-1-D nanocomposite was used to thicken the gas without the use of co-solvents.[25] Nanoparticle dispersions in CO_2 have been mainly studied at the viscometer or core flood level, and further research regarding their long-term stability is required. Lemaire et al. (2021) suggest that while there have been only a few reports of stable nanoparticle dispersion in CO_2, future research in this area with surface-functionalized silica nanoparticles with non-fluorous highly CO_2-philic ligands may be promising.[26]

Other polymers, such as P-1-D and PVEE,[27,28] have been tested as CO_2 and CO_2-rich gas thickeners. Unfortunately, P-1-D and PVEE polymers, especially at low MWs, lack consensus regarding their ability to thicken CO_2. Contradicting results and failed attempts to reproduce findings have been shown, where low-MW polymers/oligomers were unable to significantly increase CO_2's viscosity.[26] Small associative polymers were suggested[29] to be soluble in $scCO_2$. So far, at a laboratory scale, the best CO_2 thickeners are PDMS, polyFAST, and PFOA for CO_2 mobility and conformance control.[30]

Unfortunately, in order to significantly increase the viscosity of $scCO_2$, large-MW polymers are required. As their solubility decreases with increasing MW, considerable amounts of co-solvent are required to dissolve these thickeners, thus making their cost economically prohibitive. Therefore, the design of more soluble and efficient thickeners is essential for the development and implementation of the technology.

Partially cross-linked polymers were tested by Kazantsev et al. as thickeners for different solvents. Various degrees of cross-linking were tested by controlling the content of the cross-linking agent. They found that a partial degree of cross-linking achieved the greatest viscosity increment. This is due to the formation of macromolecular coils occupying the largest volume in solution. They also found that a further increase of cross-linking content in the polymer makes it insoluble.[31]

Gallo and Erdmann studied the implementation of thickened CO_2 combined with a WAG scheme, making the process economically feasible. By injecting the thickened gas within a large slug of CO_2, high volumetric efficiency can be achieved combined with high recovery factors while significantly reducing the costs of thickeners. The same research also showed that the optimal CO_2 viscosity for that study was between 0.3 and 0.5 cp. This was due to the fact that higher viscosity accounted for a higher pressure drop in the reservoir, leading to a loss of miscibility.[32] Similar results were reported where compositional reservoir simulation showed that increasing the injected gas viscosity close to that of the oil (0.24 cp) had a significant impact on oil recovery.[33]

The design of CO_2-philic additives is complex, time-consuming, and expensive due to the characteristics of this supercritical fluid. Laboratory experiments usually require long periods of experimentation, specialized apparatuses, and the testing of numerous candidates. Many current polymer candidates are custom-made, requiring polymer synthesis, making their development slow, difficult, and costly. Additionally, in some cases, the mechanisms responsible for their solubility are poorly understood.

In this study, we used a quantum mechanical (QM) solvation model to efficiently narrow down the list of thickener candidates, thus significantly reducing the testing time and cost, while having a further understanding of CO_2−polymer interactions and thus determining a more CO_2-philic additive. Viscosity enhancement was later studied using an experimental rolling ball apparatus and contrasted with nanofluids. We found that silicone resins have high CO_2-philicity as well as good viscosity enhancement capabilities.

■ MATERIALS AND METHODS

Solubility from Free Energy of Solvation. Implicit or continuous solvent models, where the solvent is represented by a polarizable dielectric continuum and its interaction with the solute is accounted for through the reaction field, offer an excellent trade-off between computing time and accuracy,

https://doi.org/10.1021/acsomega.1c03660
ACS Omega 2021, 6, 24803−24813

offering an appealing alternative to explicit models.[34,35] The conductor-like polarizable continuum model (CPCM) partitions the surface in small regions called tesserae, which are assigned partial charges based on the electrostatic potential.[36] CPCM is often considered one of the most successful solvation models[37,38] and was used to study isomeric structures, energies, and properties of the substituted silacyclopropylidenoids in various solvents.[39]

The thermodynamic cycle using the solvation free energy (ΔG_{sol}), the standard-state free energy of the liquid−vapor equilibrium of component A (ΔG_1°), and the standard-state free energy of the equilibrium of a given solvent ($scCO_2$) with liquid A (ΔG_2°) is shown in Figure 1.

$$\Delta G_1^{\circ} = RT \ln \frac{P_x^{\bullet} M^{\circ}}{P^{\circ} M_x^{s}} \tag{1}$$

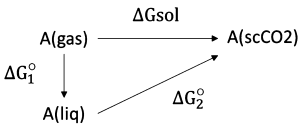

Figure 1. Thermodynamic cycle used for solubility calculations.

where the standard free energies are represented[40] as

$$\Delta G_2^{\circ} = -RT \ln \frac{S}{M_x^{s}} \tag{2}$$

where $P_x^{\bullet}$ is the equilibrium vapor pressure of X over pure X, P° is the pressure of an ideal gas at a 1 M concentration and 298 K, M° is the standard-state molarity, M_x^{s} is the equilibrium molarity of pure X, S is the solubility in molarity units, R is the gas constant, and T is the absolute temperature. $M^{\circ}$is equal to 1 mol per liter as defined in P° in order to simplify the equations. By adding eqs 1 and 2, S can be expressed in terms of ΔG_{sol} according to[41]

$$S = \frac{P_x^{\bullet} M^{\circ}}{P^{\circ}} \exp\left[\frac{-\Delta G_{sol}}{RT}\right] \tag{3}$$

Using eq 3, the relative solubility of component A with respect to a known component B can be expressed as

$$\frac{S_a}{S_b} = \frac{P_a^{\bullet}}{P_b^{\bullet}} \exp\left[\frac{\Delta G_{solb} - \Delta G_{sola}}{RT}\right] \tag{4}$$

In this paper, we used linear PDMS as a reference for comparison as it is the most soluble non-fluorinated CO_2 thickener known to date.[42]

Since the vapor pressure of polymers is usually very low and not always available, using eqs 1−3 it is expedient to express S in terms of ΔG_{sol} and ΔG_1°, that is, the free energy of solvation of component X in its liquid, according to

$$S = M_x^{s} \exp\left[\frac{-(\Delta G_{sol} - \Delta G_1^{\circ})}{RT}\right] \tag{5}$$

where M_x^{s} is obtained using the component's X density and its molar mass. Thus, the solubility increment of component A over B can be calculated as

$$\frac{S_a}{S_b} = \frac{M_a^{s}}{M_b^{s}} \exp\left[\frac{\Delta Gsol_b - \Delta Gsol_a + \Delta G_{1a}^{\circ} - \Delta G_{1b}^{\circ}}{RT}\right] \tag{6}$$

QM CPCM Solvation Model. In a continuum model, the influence of the solvent over the solute Hamiltonian ($\hat{H}$) is expressed as

$$\hat{H} = \hat{H}^{\circ} + \hat{V} \tag{7}$$

where $\hat{H}^{\circ}$ is the solute Hamiltonian in vacuum and $\hat{V}$ represents the perturbation due to the effect of the solvent. The CPCM model characterizes the solvent as a conductor-like polarizable continuum using its dielectric constant. The surface is discretized with a tessellation scheme where point charges are located in small areas (tesserae). The operator $\hat{V}$ is written in terms of these apparent polarization charges q_i placed on each tessera i. Considering the conductor-like boundary condition

$$V(\vec{r}) + \sum_{i}^{\text{tesserae}} V_{qi}(\vec{r}) = 0 \tag{8}$$

where V is the electrostatic potential due to the solute, V_{qi} is the electrostatic potential due to the polarization charges, and $\vec{r}$ is a point on the surface. The relationship between the vector of the conductor-like polarization charges (q) and V can be expressed as

$$Aq = -V \tag{9}$$

where V contains the solute electrostatic potential on the cavity surface, and matrix A (in CPCM) is defined as[43]

$$A_{ii} = \frac{\varepsilon}{\varepsilon - 1} 1.07 \sqrt{\frac{4\Pi}{S_i}} \tag{10}$$

$$A_{ij} = \frac{\varepsilon}{\varepsilon - 1} \frac{1}{|\vec{r}_i - \vec{r}_j|} \tag{11}$$

with $\vec{r}_i$ and $\vec{r}_j$ being the coordinates of tesserae i and j, respectively, ε the dielectric constant of the solvent, and S_i the area of tessera i.

The electrostatic component of the free energy of a solute in solution (G_{es}) can be written as[44]

$$G_{es} = \Psi|\hat{H}^0|\Psi + \Delta G_{es} \tag{12}$$

where ΔG_{es} is expressed as[44]

$$\Delta G_{es} = \sum_i q_i V_i(\vec{r}) + \frac{1}{2} \sum_{ij} A_{ij} q_i q_j \tag{13}$$

and V_i indicates the value of the electrostatic potential due to the solute on the ith tessera.

Calculating the total energy of the molecule in vacuum (E°), the electrostatic energy of the molecule (ΔG_{es}), and the non-electrostatic contribution (ΔG_{CD}), the solvation free energy (ΔG_{sol}) can be approximated as[45,46]

$$\Delta G_{sol} = (\Delta G_{es} + \Delta G_{CD}) - E^{\circ} \tag{14}$$

where the non-electrostatic term includes the short-range Van der Waals solute−solvent interactions and the energy needed to build the cavity (cavitation term). In order to simulate the $scCO_2$ solvent with CPCM, a dielectric constant representative of $scCO_2$ at 100 bar and 50 °C was used. In this paper, we used an experimental dielectric constant of 1.215.[47]

To study the solvation of several silicones, a CPCM model was used to calculate solvation free energies using the BP86 level of density functional theory (due to its lower computa-

https://doi.org/10.1021/acsomega.1c03660
ACS Omega 2021, 6, 24803−24813

tional cost as shown in previous studies[48]) utilizing the ORCA[49,50] quantum mechanics software.

Laboratory Rolling Ball Measurements. The rolling ball allows the measurement of fluid viscosity under reservoir conditions. This apparatus consists of a metallic ball, which falls within a tube containing the fluid at the required pressure and temperature (Figure 2). The ball is initially held magnetically in the upper section of the tube and later dropped, electronically measuring the time required to reach the sensor at the bottom end of the apparatus. The viscosity measurements presented in this paper were carried out at an apparatus tilt (θ) of 70° with a ball diameter of 0.64 cm, and the apparatus was calibrated with hexane. Viscosity tests were carried out at 180 bar and 55 °C to emulate reservoir conditions and later at different temperatures to better understand its effect on the polymer-nanofluid solution's rheology.

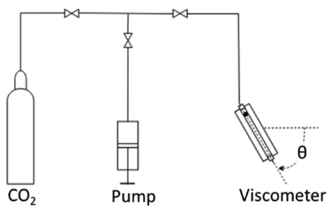

Figure 2. Rolling ball apparatus setting.

As the tube's length and ball diameter remain constant, the viscosity of the fluid can be calculated as

$$\mu = Kt(\delta_b - \delta_f) \tag{15}$$

where μ is the fluid viscosity, K is a constant unique to the set of tests, t is the time that takes the ball to roll from the top to the bottom of the apparatus, δ_b is the density of the ball, and δ_f is the density of the fluid. By comparing the rolling balls' measurement of the tested fluid with the measurements of a known fluid with similar viscosity (i.e., hexane), the tested fluid's viscosity can be calculated using the following equation:

$$\mu_t = \frac{t_t(\delta_b - \delta_f)}{t_h(\delta_b - \delta_h)}\mu_h \tag{16}$$

where μ_t is the tested fluid's viscosity, μ_h is the viscosity of hexane, t_t is the rolling time with the tested fluid, t_h is the rolling time with hexane, and δ_h is the density of hexane.

Different polymer−$scCO_2$ mixtures were tested in a Ruska rolling ball viscometer. The AK 12,500 and AK 60,000 silicone fluids were used to study linear PDMS, while Silres KX (having a proprietary molecular structure) was used to study silicone resin (Table 1). PDMS samples were chosen with similar and lower MWs than previous studies regarding silicone nanofluids[21] as they are expected to have higher solubilities in CO_2 than the high-MW silicones such as the ones used by Bae and Irani[9] and therefore require less co-solvent. While using lower-MW silicones would require higher polymer concentrations to obtain the same viscosities, the overall additive concentration is lower due to the reduced need for a co-solvent. Both linear PDMS and silicone resins were provided by Wacker Silicones. Coated nanoparticles from PlasmaChem were added to the silicones to generate nanofluids (Table 2). The nanoparticle's hydrophobic coating was chosen to assist dispersion. The AK 12,500 silicone was mixed with a 10% w/w nanoparticle concentration, while the AK 60,000 PDMS was mixed with 5, 10, and 30% w/w nanoparticle concentrations to understand the effect of the polymer's MW and nanoparticles on the $scCO_2$ viscosity. Nanoparticles were first dispersed in linear PDMS overnight using a heated ultrasonic bath. Afterward, they were prepared in an 80% m/m toluene—20% m/m polymer−nanoparticle mixture to facilitate the dissolution of the mixture in CO_2. Toluene was chosen as a co-solvent based on Bae and Irani's experiments, who benchmarked PDMS as a CO_2 thickener.[9] In order to mix the additive in carbon dioxide, the samples were left in the rolling ball apparatus for up to 3 days, heated at 80−90 °C, and with occasional rocking in order to stabilize the mixture and obtain consistent viscosity measurements.

Table 2. Nanoparticle Properties

NP type	size (nm)	coating	type of coating
silica	14	PDMS	chemically attached

■ RESULTS AND DISCUSSION

The design of $scCO_2$ thickeners was carried out in two steps. First, the relative solubilities of several silicone-based components were estimated using the CPCM solvation model to determine $scCO_2$-philicity. Afterward, the viscosity of the CO_2 solution with the chosen candidate was measured in a rolling ball apparatus and contrasted with that of PDMS of different MWs and increasing addition of nanoparticles.

Prediction of Solubility Using the CPCM Solvation Model. To understand the solubility of silicone polymers and resins in $scCO_2$, ΔG_{solv} of several silicones were calculated using CPCM solvation models in order to determine their CO_2-philicity.

Common functional silicones were modeled having six functional repeating units and two trimethyl siloxane end groups (Table 3). PDMS molecules were analyzed with different amounts of repeating units in order to contrast solubilities as a function of MW. MQ resin and silsesquioxiane were included in order to determine how different types of structures affect solubility.

Overall, the CPCM solvation model showed good agreement with the expected solubility behavior from the literature[12,13,42] and revealed itself to be a suitable method to test and design solutes for $scCO_2$. The utilization of a computational calculation significantly reduced the screening time and cost by reducing the need of purchasing or synthesizing and testing the polymers.

Table 1. Silicone Polymers

silicone (type)	viscosity (C_p)	M_w	substituent type	degree of cross-linking	main functionality	SiO_2 content
Silres AK 60,000	60,000	∼63,500	methyl			
Silres AK 12,500	12,500	∼39,500	methyl			
Silres KX	6−12 (50% wt. xylene)	8000−15,000	methyl	71%	ethoxy/silanol	88%

https://doi.org/10.1021/acsomega.1c03660
ACS Omega 2021, 6, 24803−24813

Table 3. Structure and Size of Linear Silicone Polymers

Compound	Structure	Size
1	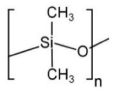	n = 5 - 11 MW = 533 - 978
2	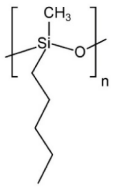	n = 6 MW = 944
3	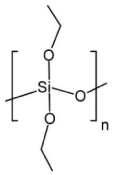	n = 6 MW = 968
4	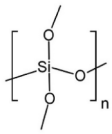	n = 6 MW = 799
5	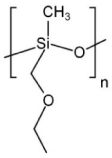	n = 6 MW = 872
6	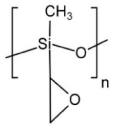	n = 6 MW = 860
7	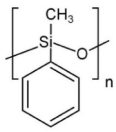	n = 6 MW = 994
8	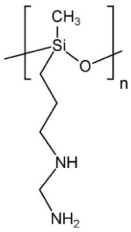	n = 6 MW = 1124

In the case of functional silicones in Table 3, only ΔG_{solv} could be calculated for many compounds due to unavailable data (vapor pressure/dielectric constant). As solubility is dependent on the difference between ΔG_{solv} and ΔG_1°, functional groups' effect on solubility could be analyzed using the vapor pressure of monomers and eq 4. Solvation free energies for linear and functional PDMS are shown in Figure 3.

As expected, linear silicones with functional groups containing oxygen or nitrogen had lower solvation free energy than the equivalent MW PDMS. Simulations show that the addition of oxygen or nitrogen enhances the electrostatic interactions with the medium, while methyl or other alkyl groups augmented ΔG_{solv}. The methoxy functional group had the highest rate of oxygen to carbon atoms and therefore was expected to have a relatively low ΔG_{solv} and higher solubility in $scCO_2$. Amino groups also appear to improve interactions with the solvent. Nonetheless, while we found that polar groups enhanced solvation, it should be noted that polar groups in the extremities of the molecules generate strong intermolecular interactions, such as hydrogen bonding, with adjacent molecules leading to poor solubility. This could explain why poly(vinyl acetate) is soluble in CO_2, while poly(acrylic acid) is not.[51] Amino groups do reduce ΔG_{solv} and are useful for carbon capture, but their hydrogen bond interaction would reduce their ability to disperse, lowering their solubility in CO_2.

While vapor pressure data for poly dimethoxy siloxane (compound 4) are not available in the literature, it is possible to infer that the vapor pressure is lower than that of PDMS comparing the vapor pressure data of tetramethoxysilane (PubChem CID: 12682)[52] and tetramethylsilane (PubChem CID: 6396).[53] Using eq 4, we see that the solubility enhancement is not significant as the exponential term is offset by the lower vapor pressure of the methoxy-functional silicone. In order to further analyze alkoxy-silicones, additional calculations for poly(MTES-*co*-TEOS) (compound 9, Table 4) were performed as the polymer's dielectric constant data are available from the literature.

Poly(MTES-*co*-TEOS) has a dielectric constant of 3.5,[54] and for linear silicones (compound 1, $n = 10$), we used a dielectric constant of 2.2.[55] ΔG_1° can be calculated with the available data, and solubility enhancement can be estimated using eq 6. As shown in Table 5, while ΔG_{solv} of alkoxy-silicones is lower than that of PDMS, it is offset by the lower ΔG_1°. Therefore, alkoxy functional silicones do not exhibit enhanced solubility in $scCO_2$. Nonetheless, their impact on solubility is moderate; therefore, having a reduced number of alkoxy groups (as happens in many silicone resins since they are used to cure them) would not significantly impact the silicone resin's solubility.

The studied resins and silsesquioxanes are shown in Table 6. They have the potential to be significantly better CO_2 thickeners than linear PDMS as their structure has a greater effect on solution viscosity. Additionally, partially cross-linked silicone rubbers are expected to be CO_2-philic as they have a similar, or even lower, solubility parameter ($\delta = 7.3–7.5$ $cal^{1/2}/cm^{3/2}$) than linear PDMS ($\delta = 7.5$ $cal^{1/2}/cm^{3/2}$).[57] These Hildebrand solubility parameters are in the range of those of $scCO_2$, which vary from 3.7 to 8 $cal^{1/2}/cm^{3/2}$ at pressures over 10 MPa.[58]

In this study, we compared the MQ silicone resin (compound 10), methyl terminated silsesquioxane (compound 11), silica gel (compound 12), and octaphenyl-silsesquioxane (compound 13) in order to understand the effect of different structures and substituent group types in solubility (Table 6).

MQ resin and linear PDMS have comparable ΔG_{solv} as they have the same amount of methyl groups per silicon and oxygen atoms. In contrast, silsesquioxane has a lower ΔG_{solv} showing that these three-dimensional structures are more CO_2-philic than linear silicones (Figure 4), in agreement with Doherty et

https://doi.org/10.1021/acsomega.1c03660
ACS Omega 2021, 6, 24803−24813

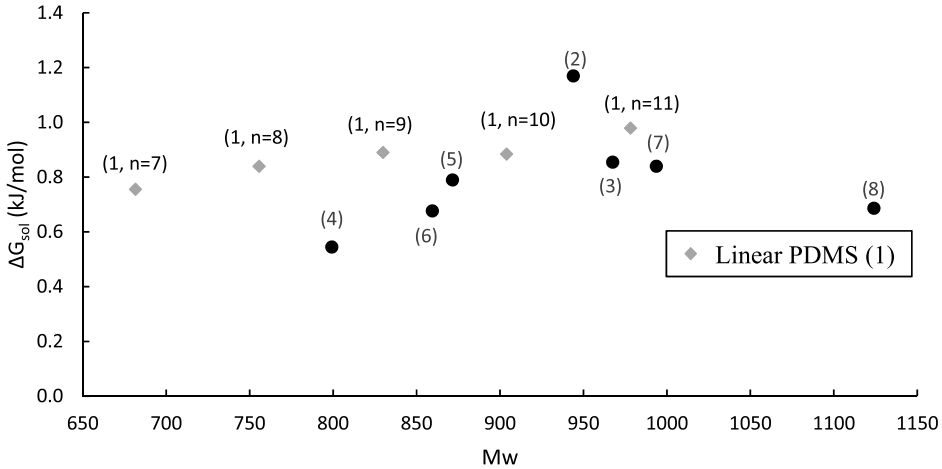

Figure 3. Solvation free energy of linear silicones. (●) represent functional silicones as numbered in Table 3, and ( ) represent linear PDMS of different MWs.

Table 4. Structure of poly(MTES-*co*-TEOS)

Compound	Structure	Size
9 poly(MTES-co-TEOS)	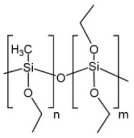	n = 3 m=3 Mw = 877

al.[12] findings. Silsesquioxanes have a lower ΔG_{solv} due to the higher silicone oxide to methyl ratio, while having non-polar groups in the extremities of the molecule. As expected, silica (compound 12) has even lower solvation free energy due to the hydroxyl group, which adds to the polarity of the molecule enhancing the electrostatic interaction with the medium. Unfortunately, as discussed for amine functional groups, the hydrogen bonding of the hydroxyl group would account for higher intermolecular interactions, diminishing their solubility.

Solubility enhancement of methyl and phenyl silsesquioxanes was estimated using eq 6. For PDMS (compound 1, $n = 5$ and $n = 11$), silsesquioxane (compound 11), and octaphenylsilsesquioxane (compound 13), we used dielectric constants of 2.2,[55] 2.6,[59] and 2.8,[60] respectively. While the exponential term of the solubility comparison of silsesquioxane and PDMS in eq 6 is slightly lower than 1, the higher density,[55,61] and therefore higher molarity of silsesquioxane, determines that they are 20% more soluble than linear PDMS of a similar MW (Table 7). In contrast, phenyl groups are found to reduce silsesquioxane's solubility in $scCO_2$.

It is observed that polar groups (e.g., Si−O) are beneficial for reducing ΔG_{solv}; nonetheless, having polar groups on the external part of the molecule could be detrimental to their solubility as they increase intermolecular interactions. By increasing polar groups within the internal part of the molecule while having non-polar groups (e.g., methyl) in the outer layer of the molecule, reducing intermolecular interactions, solubility is enhanced. Due to this, silsesquioxanes are predicted to be more soluble than linear PDMS, the leading CO_2 thickening polymer so far,[42] and functional silicones. Methyl silicone resins also have good rheological properties, commercial availability, non-reactivity, and a moderate cost.

Table 6. Structure and Size of Resins and Silsesquioxanes

Compound	Structure	Size
10 MQ Resin	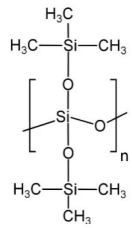	n = 2 MW = 607
11 Silsesquioxane	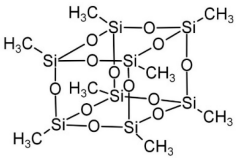	MW = 537
12 Silica gel	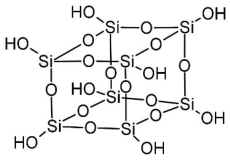	MW = 552
13 Octaphenyl-silsesquioxane	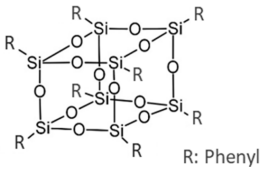	MW = 1034

Table 5. Solubility Increment of Alkoxy-Silicone over PDMS

	density (g/cm^3)	M_w (g/mol)	M^s (mol/cm^3)	ΔG_{solv} (J/mol)	ΔG_1 (J/mol)	Spoly(MTES-co-TEOS)/SPDMS
poly (MTES-*co*-TEOS)	1.06[56]	877	0.0012	814	−186	0.94
PDMS (n = 10)	0.97[55]	904	0.0011	884	331	

https://doi.org/10.1021/acsomega.1c03660
ACS Omega 2021, 6, 24803−24813

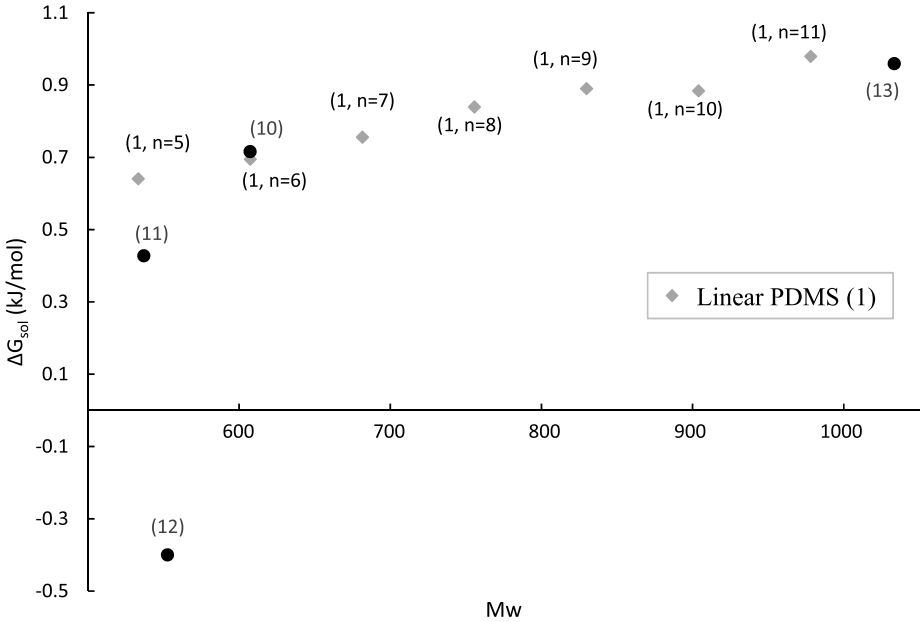

Figure 4. Solvation free energy of resins and silsesquioxanes. (●) represent compounds as numbered in Table 6, and ( ) represent linear PDMS of different MWs.

Table 7. Solubility Increment of Silsesquioxanes over PDMS

	density (g/cm^3)	MW (g/mol)	M^s (mol/l)	ΔG_{solv} (j/mol)	ΔG_1 (j/mol)	Ssilsesquioxane/SPDMS
silsesquioxane	1.27[61]	537	2.4	427	−194	1.20
PDMS (n = 5)	0.97[55]	533	1.8	695	283	
octaphenyl-silsesquioxane	1.3[61]	1034	1.3	959	−531	0.88
PDMS (n = 11)	0.97[55]	978	1.0	979	408	

Table 8. Thickened CO_2 Viscosity Measured at 55 °C and 180 bar

additive	type	silicone (mg)	NP (mg)	concentration (m/m %) in CO_2	viscosity (cp)
1	pure CO_2				0.06[62]
2	AK 12,500	720	80	5.60	0.3
3	AK 12,500	560	240	5.60	unstable
4	AK 60,000	800	0	5.60	0.27
5	AK 60,000	760	40	5.60	0.38
6	AK 60,000	720	80	5.60	0.54
7	AK 60,000	560	240	5.60	unstable
8	AK 60,000 (without toluene)	950	50	6.90	0.5
9	KX resin	1000	0	6.90	0.25
10	KX resin	900	100	6.90	0.24
11	NPs (with toluene)	0	650	4.50	unstable

Viscosity Measurements Using the Rolling Ball. Solubility in $scCO_2$ and viscosity enhancement are the two fundamental properties looked for in CO_2 thickeners. Computational methods can be used to understand solvation and solubility in order to do a fast additive screening. Unfortunately, state-of-the-art computational (molecular dynamics) viscosity calculations for these types of systems are not as reliable. Therefore, solution viscosities of the narrowed-down candidates were measured directly in the laboratory through rolling ball experiments, which provide not only direct viscosity measurements but also indirect qualitative information of solubility and quickness of the solute−solvent mixture through the time taken to stabilize measurements. Unfortunately, we were not capable of conducting direct visual observation of the mixtures due to the lack of availability of the appropriate equipment. Further research utilizing windowed cells should be carried out in future work to verify the occurrence and long-term stability of a single phase in order to corroborate the findings presented in this paper.

As previously stated by the solubility screening, silicones with branched/cage-like structures with methyl substituent groups appear to be the most promising candidates. We continued by measuring CO_2 with methyl silicone resin mixture viscosity and compared it to PDMS-based nanofluids. In order to compare thickening capability, we prepared nanofluids with two linear silicones of different MWs and increasing concentrations of hydrophobic silica nanoparticles (Table 8). Viscosity measurements of commercial silicone resin and PDMS (with and without nanoparticles) dispersed in $scCO_2$ were tested in a rolling ball apparatus at 180 bar and 55 C and calculated using eq 16.

https://doi.org/10.1021/acsomega.1c03660
ACS Omega 2021, 6, 24803−24813

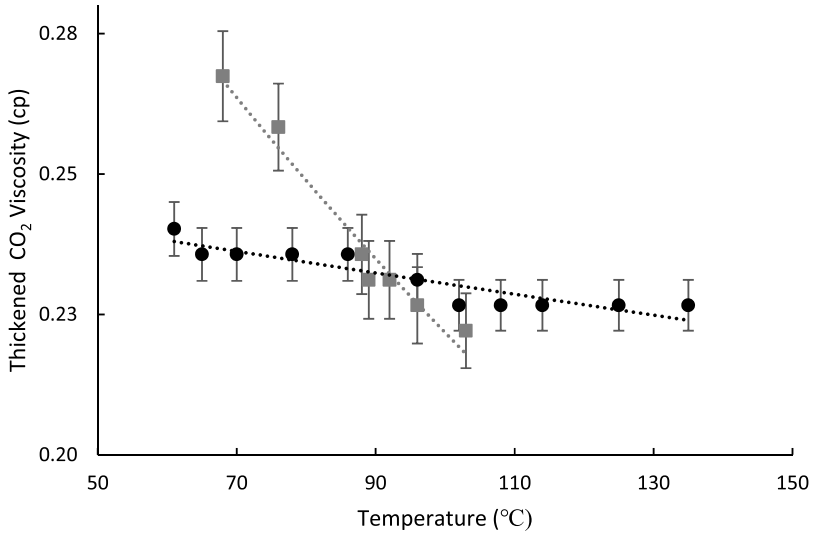

Figure 5. Viscosity of thickened CO_2 with nanofluids and resins at different temperatures. (●) represent silicone resin (additive 9 as numbered in Table 8), and ( ) represent PDMS with 5% NP (additive 5 as numbered in Table 8).

Within the MW range of these experiments, the viscosity of the CO_2-based nanofluid increased with the linear polymer's MW as well as with nanoparticle concentration. In the case of resins, nanoparticle addition had an opposite effect on viscosity. This could be due to the reduction in the overall resin concentration. Nanoparticles alone, without the addition of polymers, did not significantly increase the mixtures viscosity and were unstable. It appears that while nanoparticles do not have a direct effect on the solution's viscosity, they enhance the thickening capacity of PDMS by aiding the creation of networks capable of further increasing viscosity. Due to the structure of resins, nanoparticles appear not to aid the formation of networks and have no significant effect on viscosity.

All readings from linear silicones with and without nanoparticles (additives 2–8, Table 8) required hours or even days of rocking at high temperatures (80–90 °C for mixing, which was further lowered to reach experimental conditions) to stabilize, even with large concentrations of co-solvent. Increasing MW and nanoparticle concentration also affected the difficulty of stabilizing measurements as compound 6 took the longest to stabilize. Since PDMS additives required such long times to stabilize, even though some eventually showed steady readings, their long-term stability should be further studied. Also, the nanofluid additive formed clumps in the apparatus when the gas was released and the pressure dropped, leading to doubts on their stability at lower pressures (e.g., within production wells or their vicinity). Larger concentrations of nanoparticles lead to higher formation of clumps in the apparatus. This may be due to the fact that higher concentrations of nanoparticles increase the probability of aggregation.[63] On the other hand, for methyl-silicone resins [additives 9 and 10 (Table 8), which are analogues of compound 11 (Table 6)], viscosity measurements stabilized very fast (within seconds) without the need of rocking or increasing the system temperature and showed no signs of clumping as the gas was vented from the apparatus. As silicone resins stabilized significantly faster than linear PDMS, even with a lower co-solvent concentration, it qualitatively implies that they mix more rapidly and are significantly more soluble in $scCO_2$ than the linear PDMS. This is aligned with the findings of the QM simulations, where the higher degree of Si–O bonds reduced the solvation free energy of silicone resins, while the outer methyl/methyl-siloxy groups aid the intermolecular repulsion, improving their solubility. It is also notable that the silicone resin showed a similar viscosity increment to linear silicones (AK 60,000) while having over 5 times lower MW. In addition, the viscosity effect of PDMS and nanoparticles (additive 5) decreased with temperature, reaching 0.27 cp at 68 °C and 0.23 cp at 90 °C. On the other hand, the viscosity of resin-thickened CO_2 was very stable with temperature, decreasing only down to 0.23 cp at 135 °C from 0.25 cp at 55 °C (Figure 5).

Therefore, resins attained the targeted range of viscosities analyzed in previous studies,[32] which would ensure miscible conditions (with a moderate pressure drop) and optimize volumetric sweep efficiency. Higher CO_2 viscosities, than targeted, would lead to a significant pressure drop in the reservoir which could endanger microscopic sweep efficiency as the system falls below minimum miscibility pressure. The good rheological properties, even at high temperatures, and the enhanced solubility of silicone resins confirm that they are better CO_2 thickeners than PDMS (even when nanoparticles are added to the linear silicones)

While using resins, it is advisable to consider their size in comparison to the reservoir's rock pore throat diameter. The relatively low MW of the Silres KX resin would ensure compatibility with most reservoir rocks and achieve appropriate viscosity increments for low- to medium-permeability reservoirs. Nonetheless, larger-MW silicone resins may be used in higher-permeability reservoirs, where more viscous CO_2 may be required, as they have larger pore throat diameters.

Resins can also have a significant impact in shale reservoirs (shale EOR and dry-fracking) where the viscous fluid is meant to travel through fractures and small pore throat diameters are not a limitation. Therefore, higher-MW silicone resin polymers can be utilized since the size of the resin would not be an issue. In the case of unconventional EOR, the thickened gas could enhance conformance through the fractured network, while only neat CO_2 (no polymer) would enter the matrix.

While bibliography suggests the use of a co-solvent to increase the solubility of PDMS,[9] we observed that the used

https://doi.org/10.1021/acsomega.1c03660
ACS Omega 2021, 6, 24803–24813

PDMS and nanoparticles were sufficiently soluble in $scCO_2$ (additive 8, table 8). This may be due to the use of a lower-MW silicone than previously used in other papers. However, like with all linear PDMS additives, it required rocking for long periods at high temperatures to stabilize.

We found that at high nanoparticle concentrations, nanoparticles in both toluene and PDMS were unstable. While the fluid viscosity was apparently increased, the readings were not even and therefore unreliable. It was later confirmed that the nanoparticles coalesced and agglomerated, forming a gel-like fluid that obstructed the viscometer's inner tube. It was also observed that this phenomenon increased as a function of time. While this could be attributed to the nanoparticle concentration and type, it is suggested to study nanoparticle behavior for each specific case taking all conditions (e.g., lower pressure and temperature at producer wells) into consideration.

CONCLUSIONS

In this paper, a novel approach for CO_2-philic thickener design was developed. Solubility comparison from QM calculations using an implicit solvent model of several PDMSs, functional linear silicones, and silsesquioxanes was used to screen candidates and further understand solubility mechanisms. Subsequently, the viscosities of CO_2 solutions with linear silicones and resins with the addition of nanoparticles were measured using a rolling ball apparatus. Effective thickeners were developed in a more efficient manner, achieving a target viscosity of 0.25−0.5 cp, which is believed to be optimal for many CO_2 EOR implementations.

The QM solvation model was shown to be a suitable method for fast screening of soluble compound candidates by determining relative solubility in $scCO_2$ prior to laboratory testing, significantly reducing the time of polymer design. Computational methods allow for flexibility in the molecular design and do not require the synthesis of every candidate. Candidates' solubilities can be further understood and compared using available polymer/monomer data. Whenever reliable vapor pressures were not available, we introduced a method for estimating polymer solubility in CO_2 by calculating ΔG_{solv} and the solvation free energy of the candidate in its liquid (ΔG_l°).

Different silicone-based polymers (with addition of toluene) may serve as useful CO_2 additives and help disperse PDMS-coated silica nanoparticles. Nanoparticles appear to enhance PDMS capacity to thicken CO_2, although the same results were not observed when added to silicone resins.

Methyl silicone resins were found to be efficient CO_2 thickeners as they are more soluble and have better rheological properties than linear PDMS. They have a higher impact on solution viscosity than linear PDMS, achieving target viscosities at a lower MW and at a wide range of temperatures. Not only they are better thickeners but also silicone resins have a low cost and are commercially available, making them an economically viable solution.

This opens the door for future research with different types and MWs of silicone resins. As unconventional resources are not limited by small pore-throat diameters in the fractures, significantly higher-MW resins could also be used to control CO_2 viscosity in shale EOR or dry-fracking operations. While promising, further research in windowed vessels should be carried out to further validate the solubility and stability of resins and PDMS nanofluids in $scCO_2$. Further core flood experiments would also be required in order to understand rock−fluid interactions such as polymer adsorption and apparent viscosity in different porous mediums.

AUTHOR INFORMATION

Corresponding Author

Claudio N. Cavasotto − *Computational Drug Design and Biomedical Informatics Laboratory, Instituto de Investigación en Medicina Traslacional (IIMT), Universidad Austral-CONICET, B1629 Pilar, Buenos Aires, Argentina; Austral Institute for Applied Artificial Intelligence and Facultad de Ingeniería, and Facultad de Ciencias Biomédicas, Universidad Austral, B1629 Pilar, Buenos Aires, Argentina;* orcid.org/0000-0002-1372-0379; Email: CCavasotto@austral.edu.ar

Authors

Gonzalo Gallo − *Instituto Tecnológico de Buenos Aires (ITBA), C1106 Buenos Aires, Argentina*

Eleonora Erdmann − *Instituto de Investigaciones para la Industria Química (INIQUI), A4400 Salta, Argentina; Consejo Nacional de Investigaciones Científicas y Técnicas (CONICET), C1425 Buenos Aires, Argentina; Universidad Nacional de Salta (UNAS), A4400 Salta, Argentina*

Complete contact information is available at: https://pubs.acs.org/10.1021/acsomega.1c03660

Notes

The authors declare no competing financial interest.

ACKNOWLEDGMENTS

Silicone fluids and resins were donated by Safer SACIF, Argentina.

REFERENCES

(1) Tiffin, D. L.; Yellig, W. F. Effects of Mobile Water on Multiple-Contact Miscible Gas Displacements. *Soc. Pet. Eng. J.* **1983**, *23*, 447−455.

(2) Shyeh-Yung, J.-G. J. Mechanisms of Miscible Oil Recovery: Effects of Pressure on Miscible and Near-Miscible Displacements of Oil by Carbon Dioxide. *SPE Annual Technical Conference and Exhibition*; SPE, 1991.

(3) Lin, E. C.; Huang, E. T. S. The Effect of Rock Wettability on Water Blocking During Miscible Displacement. *SPE Reservoir Eng.* **1990**, *5*, 205−212.

(4) Stern, D. Mechanisms of Miscible Oil Recovery: Effects of Pore-Level Fluid Distribution. *SPE Annual Technical Conference and Exhibition*; SPE, 1991.

(5) Shelton, J. L.; Schneider, F. N. The Effects of Water Injection on Miscible Flooding Methods Using Hydrocarbons and Carbon Dioxide. *Soc. Pet. Eng. J.* **1975**, *15*, 217−226.

(6) Rogers, J. D.; Grigg, R. B. A Literature Analysis of the WAG Injectivity Abnormalities in the CO2 Process. *SPE/DOE Improved Oil Recovery Symposium*; SPE, 2000.

(7) Jarrell, P. M.; Fox, C.; Stein, M.; Webb, S. Practical Aspects of CO2 Flooding; Society of Petroleum Engineers, SPE Monograph Series Vol. *22*, 26, 2002.

(8) Enick, R. M.; Olsen, D. K.; Ammer, J. R.; Schuller, W. Mobility and Conformance Control for CO2 EOR via Thickeners, Foams, and Gels -- A Literature Review of 40 Years of Research and Pilot Tests. *SPE Improved Oil Recovery Symposium*; SPE: Tulsa, 2012.

(9) Bae, J. H.; Irani, C. A. A Laboratory Investigation of Viscosified CO2 Process. *SPE Adv. Technol.* **1993**, *1*, 166−171.

(10) Dai, C.; Wang, T.; Zhao, M.; Sun, X.; Gao, M.; Xu, Z.; Guan, B.; Liu, P. Impairment Mechanism of Thickened Supercritical Carbon Dioxide Fracturing Fluid in Tight Sandstone Gas Reservoirs. *Fuel* **2018**, *211*, 60−66.

(11) O'Brien, M. J.; Perry, R. J.; Doherty, M. D.; Lee, J. J.; Dhuwe, A.; Beckman, E. J.; Enick, R. M. Anthraquinone Siloxanes as Thickening Agents for Supercritical CO2. *Energy Fuels* **2016**, *30*. DOI: 10.1021/acs.energyfuels.6b00946.

(12) Doherty, M. D.; Lee, J. J.; Dhuwe, A.; O'Brien, M. J.; Perry, R. J.; Beckman, E. J.; Enick, R. M. Small Molecule Cyclic Amide and Urea Based Thickeners for Organic and Sc-CO2/Organic Solutions. *Energy Fuels* **2016**, *30*, 5601−5610.

(13) Wang, Y.; Li, Q.; Dong, W.; Li, Q.; Wang, F.; Bai, H.; Zhang, R.; Owusu, A. B. Effect of Different Factors on the Yield of Epoxy-Terminated Polydimethylsiloxane and Evaluation of CO2 Thickening. *RSC Adv.* **2018**, *8*, 39787−39796.

(14) Li, Q.; Wang, Y.; Wang, X.; Yu, H.; Li, Q.; Wang, F.; Bai, H.; Forson, K. An Application of Thickener to Increase Viscosity of Liquid CO 2 and the Assessment of the Reservoir Geological Damage and CO 2 Utilization. *Energy Sources, Part A Recovery, Util. Environ. Eff.* **2019**, *41*, 368−377.

(15) Li, Q.; Wang, Y.; Wang, F.; Li, Q.; Kobina, F.; Bai, H.; Yuan, L. Effect of a Modified Silicone as a Thickener on Rheology of Liquid CO2 and Its Fracturing Capacity. *Polymers* **2019**, *11* (). https://doi.org/ DOI: 10.3390/polym11030540.

(16) Zhang, Y.; Zhu, Z.; Tang, J. Investigation on Modified Polyether as Efficient CO2 Thickener. *New J. Chem.* **2020**, *45*, 651−656.

(17) Xu, J.; Enick, R. M. Thickening Carbon Dioxide with the Fluoroacrylate-Styrene Copolymer. *SPE Annual Technical Conference and Exhibition*; SPE: New Orleans, 2001.

(18) Huang, Z.; Shi, C.; Xu, J.; Kilic, S.; Enick, R. M.; Beckman, E. J. Enhancement of the Viscosity of Carbon Dioxide Using Styrene/Fluoroacrylate Copolymers. *Macromolecules* **2000**, *33*, 5437−5442.

(19) Zhou, M.; Tu, H.; He, Y.; Peng, P.; Liao, M.; Zhang, J.; Xu, X.; He, W.; Zhao, Y.; Guo, X. Synthesis of an Oligomeric Thickener for Supercritical Carbon Dioxide and Its Properties. *J. Mol. Liq.* **2020**, *312*, 113090.

(20) Yousefvand, H. A.; Jafari, A. Stability and Flooding Analysis of Nanosilica/ NaCl /HPAM/SDS Solution for Enhanced Heavy Oil Recovery. *J. Pet. Sci. Eng.* **2018**, *162*. https://doi.org/ DOI: 10.1016/j.petrol.2017.09.078.

(21) Shah, R. D. Application of Nanoparticle Saturated Injectant Gases for EOR of Heavy Oils. *SPE Annual Technical Conference and Exhibition*; SPE: New Orleans, 2009.

(22) Hashemi, S. I.; Fazelabdolabadi, B.; Moradi, S.; Rashidi, A. M.; Shahrabadi, A.; Bagherzadeh, H. On the Application of NiO Nanoparticles to Mitigate in Situ Asphaltene Deposition in Carbonate Porous Matrix. *Appl. Nanosci.* **2016**, *6*, 71−81.

(23) Jafari, S.; Khezrnejad, A.; Shahrokhi, O.; Ghazanfari, M. H.; Vossoughi, M. Experimental Investigation of Heavy Oil Recovery by Continuous/WAG Injection of CO_2 Saturated with Silica Nanoparticles. *Int. J. Oil Gas Coal Technol.* **2015**, *9*, 169−179.

(24) Dezfuli, M. G.; Jafari, A.; Gharibshahi, R. Optimum Volume Fraction of Nanoparticles for Enhancing Oil Recovery by Nanosilica/Supercritical CO2 Flooding in Porous Medium. *J. Pet. Sci. Eng.* **2020**, *185*, 106599.

(25) Gandomkar, A.; Sharif, M. Nano Composites Performance as Direct Thickeners for Gas Based Enhanced Oil Recovery, a New Approach. *J. Pet. Sci. Eng.* **2020**, *194*, 107491.

(26) Lemaire, P. C.; Alenzi, A.; Lee, J. J.; Beckman, E. J.; Enick, R. M. Thickening CO2 with Direct Thickeners, CO2-in-Oil Emulsions, or Nanoparticle Dispersions: Literature Review and Experimental Validation. *Energy Fuels* **2021**, *35*, 8510−8540.

(27) Al Hinai, N. M.; Saeedi, A.; Wood, C. D.; Valdez, R.; Esteban, L. Experimental Study of Miscible Thickened Natural Gas Injection for Enhanced Oil Recovery. *Energy Fuels* **2017**, *31*, 4951−4965.

(28) Al Hinai, N. M.; Saeedi, A.; Wood, C. D.; Myers, M.; Valdez, R.; Sooud, A. K.; Sari, A. Experimental Evaluations of Polymeric Solubility and Thickeners for Supercritical CO2 at High Temperatures for Enhanced Oil Recovery. *Energy Fuels* **2018**, *32*, 1600−1611.

(29) Lee, J.; Dhuwe, A.; Cummings, S. D.; Beckman, E. J.; Enick, R. M.; Doherty, M.; O'Brien, M.; Perry, R.; Soong, Y.; Fazio, J.; McClendon, T. R. Polymeric and Small Molecule Thickeners for CO2, Ethane, Propane and Butane for Improved Mobility Control. *SPE Improved Oil Recovery Conference*; SPE: Tulsa, 2016.

(30) Al Hinai, N. M.; Myers, M.; Wood, C.; Saeedi, A. Direct Gas Thickener. In *Enhanced Oil Recovery Processes - New Technologies*; Samsuri, A., Ed.; IntechOpen, 2019.

(31) Kazantsev, O.; Rumyantsev, M. S.; Rumyantsev, M.; Savinova, M.; Khokhlova, T.; Danov, S.; Sadikov, A. Synthesis of polyacryl thickeners by radical precipitation polymerization. *Bulletin South Ural State Univ. Ser Chem.* **2015**, *15*, 52−58.

(32) Gallo, G.; Erdmann, E. Simulation of Viscosity Enhanced CO2 Nanofluid Alternating Gas in Light Oil Reservoirs. *SPE Latin America and Caribbean Petroleum Engineering Conference*; SPE, 2017.

(33) Hinai, N. M. A.; Saeedi, A.; Wood, C. D.; Valdez, R. A Numerical Study of Using Polymers to Improve the Gas Flooding in the Harweel Cluster. *SPE Reservoir Characterisation and Simulation Conference and Exhibition*; SPE, 2017.

(34) Anisimov, V. M.; Cavasotto, C. N. Hydration Free Energies Using Semiempirical Quantum Mechanical Hamiltonians and a Continuum Solvent Model with Multiple Atomic-Type Parameters. *J. Phys. Chem. B* **2011**, *115*, 7896−7905.

(35) Bordner, A. J.; Cavasotto, C. N.; Abagyan, R. A. Accurate Transferable Model for Water, n-Octanol, and n-Hexadecane Solvation Free Energies. *J. Phys. Chem. B* **2002**, *106*, 11009−11015.

(36) Gwee, E. S. H.; Seeger, Z. L.; Appadoo, D. R. T.; Wood, B. R.; Izgorodina, E. I. Influence of DFT Functionals and Solvation Models on the Prediction of Far-Infrared Spectra of Pt-Based Anticancer Drugs: Why Do Different Complexes Require Different Levels of Theory? *ACS Omega* **2019**, *4*, 5254−5269.

(37) Takano, Y.; Houk, K. N. Benchmarking the Conductor-like Polarizable Continuum Model (CPCM) for Aqueous Solvation Free Energies of Neutral and Ionic Organic Molecules. *J. Chem. Theory Comput.* **2005**, *1*, 70−77.

(38) Skyner, R. E.; McDonagh, J. L.; Groom, C. R.; van Mourik, T.; Mitchell, J. B. O. A Review of Methods for the Calculation of Solution Free Energies and the Modelling of Systems in Solution. *Phys. Chem. Chem. Phys.* **2015**, *17*, 6174−6191.

(39) Burak Yildiz, C.; Azizoglu, A. Substituent and Solvent Effects on the Electronic and Structural Properties of Silacyclopropylidenoids. *J. Mex. Chem. Soc.* **2015**, *59*, 24−28.

(40) Prediction of Vapor Pressures from Self-Solvation Free Energies Calculated by the SM5 Series of Universal Solvation Models. *J. Phys. Chem. B*, 2021; Vol. *104*, 19, pp 4726−4734 https://pubs.acs.org/doi/abs/10.1021/jp992435i (accessed 2021-04-11).

(41) Thompson, J. D.; Cramer, C. J.; Truhlar, D. G. Predicting Aqueous Solubilities from Aqueous Free Energies of Solvation and Experimental or Calculated Vapor Pressures of Pure Substances. *J. Chem. Phys.* **2003**, *119*, 1661−1670.

(42) Peach, J.; Eastoe, J. Supercritical Carbon Dioxide: A Solvent like No Other. *Beilstein J. Org. Chem.* **2014**, *10*, 1878−1895.

(43) Cossi, M.; Barone, V. Separation between Fast and Slow Polarizations in Continuum Solvation Models. *J. Phys. Chem. A* **2000**, *104*, 10614−10622.

(44) Barone, V.; Cossi, M. Quantum Calculation of Molecular Energies and Energy Gradients in Solution by a Conductor Solvent Model. *J. Phys. Chem. A* **1998**, *102*, 1995−2001.

(45) Truong, T. N.; Stefanovich, E. V. A New Method for Incorporating Solvent Effect into the Classical, Ab Initio Molecular Orbital and Density Functional Theory Frameworks for Arbitrary Shape Cavity. *Chem. Phys. Lett.* **1995**, *240*, 253−260.

(46) Cavasotto, C. N.; Aucar, M. G.; Adler, N. S. Computational Chemistry in Drug Lead Discovery and Design. *Int. J. Quantum Chem.* **2019**, *119*, No. e25678.

(47) Moriyoshi, T.; Kita, T.; Uosaki, Y. Static Relative Permittivity of Carbon Dioxide and Nitrous Oxide up to 30 MPa. *Berichte Bunsenges. Für Phys. Chem.* **1993**, *97*, 589−596.

(48) Klamt, A.; Moya, C.; Palomar, J. A Comprehensive Comparison of the IEFPCM and SS(V)PE Continuum Solvation Methods with

the COSMO Approach. *J. Chem. Theory Comput.* **2015**, *11*, 4220−4225.
(49) Neese, F. The ORCA Program System. *Wiley Interdiscip. Rev.: Comput. Mol. Sci.* **2012**, *2*, 73−78.
(50) Neese, F. *Software Update: The ORCA Program System*, version 4.0. *Wiley Interdiscip. Rev.: Comput. Mol. Sci.* 2018, *8* (1), e1327. DOI: 10.1002/wcms.1327
(51) Rindfleisch, F.; DiNoia, T. P.; McHugh, M. A. Solubility of Polymers and Copolymers in Supercritical CO2. *J. Phys. Chem.* **1996**, *100*, 15581−15587.
(52) PubChem. Tetramethoxysilane https://pubchem.ncbi.nlm.nih.gov/compound/12682 (accessed 2020-11-27).
(53) PubChem. Tetramethylsilane https://pubchem.ncbi.nlm.nih.gov/compound/6396 (accessed 2020-11-27).
(54) Gunji, T.; Tozune, T.; Kaburaki, H.; Arimitsu, K.; Abe, Y. Preparation of Co-Polymethyl(Alkoxy)Siloxanes by Acid-Catalyzed Controlled Hydrolytic Copolycondensation of Methyl(Trialkoxy)-Silane and Tetraalkoxysilane. *J. Polym. Sci. Polym. Chem.* **2013**, *51*, 4732−4741.
(55) Mark, J. E. *Polymer Data Handbook*; Oxford University Press, 1999; p 425.
(56) Poly(diethoxysiloxane), 68412-37-3 http://www.chemcd.com/prodetailCCD00051506.html (accessed 2021-08-22).
(57) Watanabe, H.; Miyauchi, T. Determination of Solubility Parameter for Siloxane Segment. *J. Chem. Eng. Jpn.* **1973**, *6*, 109−114.
(58) Marcus, Y. Solubility Parameter of Carbon Dioxide—An Enigma. *ACS Omega* **2018**, *3*, 524−528.
(59) Ahmad, Z. Polymer Dielectric Materials; IntechOpen. Available from: https://www.intechopen.com/books/dielectric-material/polymer-dielectric-materials.
(60) Cherunilam, J. F.; Rajani, K. V.; McCoy, A.; Heise, A.; Daniels, S. Investigation of O2 and SF6 Plasma Interactions on Thermally Stable Damage Resistant Poly Phenyl-Methyl Silsesquioxane Low-k Films. *J. Phys. Appl. Phys.* **2014**, *47*, 105204.
(61) 17865-85-9 CAS MSDS (Octamethylsilsesquioxane) Melting Point Boiling Point Density CAS Chemical Properties https://www.chemicalbook.com/ChemicalProductProperty_US_CB6500269.aspx (accessed 2020-11-27).
(62) Fenghour, A.; Wakeham, W. A.; Vesovic, V. The Viscosity of Carbon Dioxide. *J. Phys. Chem. Ref. Data* **1998**, *27*, 31.
(63) Rosická, D.; Šembera, J. Changes in the Nanoparticle Aggregation Rate Due to the Additional Effect of Electrostatic and Magnetic Forces on Mass Transport Coefficients. *Nanoscale Res. Lett.* **2013**, *8*, 20.

https://doi.org/10.1021/acsomega.1c03660
ACS Omega 2021, 6, 24803−24813